Electrorotation in graded colloidal suspensions

J. P. Huang

Department of Physics, The Chinese University of Hong Kong, Shatin, New Territories, Hong Kong
and Biophysics and Statistical Mechanics Group, Laboratory of Computational Engineering, Helsinki University of Technology,
P.O. Box 9203, FIN-02015 HUT, Finland

K. W. Yu

Department of Physics, The Chinese University of Hong Kong, Shatin, New Territories, Hong Kong

G. Q. Gu

Department of Physics, The Chinese University of Hong Kong, Shatin, New Territories, Hong Kong
and College of Information Science and Technology, East China Normal University, Shanghai 200 062, China

Mikko Karttunen

Biophysics and Statistical Mechanics Group, Laboratory of Computational Engineering, Helsinki University of Technology,
P.O. Box 9203, FIN-02015 HUT, Finland

Biological cells can be treated as composites of graded material inclusions. In addition to biomaterials, graded composites are important in more traditional materials science. In this paper, we investigate the electrorotation spectrum of a graded colloidal suspension in an attempt to discuss its dielectric properties. For that, we use the recently obtained differential effective dipole approximation and generalize it for nonspherical particles. We find that variations in the conductivity profile may make the characteristic frequency redshifted and have also an effect on the rotation peak. On the other hand, variations in the dielectric profile may enhance the rotation peak, but do not have any significant effect on the characteristic frequency. In the end, we apply our theory to fit experimental data obtained for yeast cells and find good agreement.

I. INTRODUCTION

Alternating current electrokinetic phenomena, i.e., electrorotation, dielectrophoresis, and traveling wave dielectrophoresis, have gained an increasing amount of attention during the past decade. This is due to their wide range of applications from cancer research to identifying and separating parasites, cell populations, and viruses [1,2], and even to design of nanomotors [3,4]. Despite the number of applications, there is a need for a theory that treats the different aspects of electrokinetic phenomena on an equal footing starting from the general underlying physical principles [5].

In this paper, we concentrate on electrorotation. Electrorotation (ER) is a phenomenon in which an interaction between a rotating ac electric field [6–8] and suspended dielectric particles leads to a rotational motion of the particles. This phenomenon was first observed experimentally over four decades ago [9] and during the past two decades, ER has been increasingly employed as a sensitive tool for noninvasive studies of a broad variety of microparticles, ranging from living cells to spores, seeds as well as synthetic materials [6,10–14].

In electrorotation, a rotating ac electric field induces a dipole moment inside a polarizable particle that rotates at the angular frequency of the external field. If the frequency of the field increases, the period of the rotating field becomes comparable to the time scale related to the formation of a dipole. To minimize its energy, the dipole tries to line up with the field but at high frequencies the particle is no longer

able to follow the field. This leads to a lag in its response and a torque is induced by the interaction of the out-of-phase part of the induced dipole moment and the external field. The torque and, in turn, the rotating speed are proportional to the imaginary part of the dipole factor (also called Clausius-Mossotti factor). In addition, the rotating speed of a particle is inversely proportional to the dynamic viscosity, since the particle is suspended in a viscous medium and experiences a dissipative drag force.

Different models have been suggested and used for analyzing experimental results, see, e.g., Refs. [5,15] and references therein. The most commonly used ones are the so-called shell models. This approach was first used by Fricke already in 1925 [16]. A model for a biological cell consisting of a single spherical dielectric shell was introduced by Arnold and Zimmermann in 1982 to investigate the rotation of a mesophyll protoplast [6]. Four years later, a two-layer model consisting of two spherical shells is put forth to discuss the electrorotation of a single plant cell [17]. Due to the inhomogeneous compartmentalization of cells, three-shell models have been used to investigate ER of liposomes [5].

These inhomogeneities can be studied in the framework of graded materials, i.e., materials with spatial gradients in their structure. Biomaterials such as cells and bones are typical examples as their composition varies through the object. Gradations can also be used to control and improve the strength and other properties, for a recent review, see Ref. [18]. In biological and medical applications, identification and separation of graded objects in micron scale (and below)

is of great importance. In these situations gradation is generic due to inhomogeneous compartments of cells, the cytoplasm often contains organelles or vacuoles. These inhomogeneities are reflected in their dielectric properties. Since differences and changes in the dielectric properties are intimately related to physical and chemical properties of cells (as well as other objects), electrorotation and other electrokinetic phenomena allow identification of particles and detection of compositional changes.

As far as one decade ago, Freyria *et al.* observed a graded cell response when they experimentally studied cell-implant interactions [19]. Recently, motivated by positional information of protein molecules, Honda and Mochizuki performed computer simulations of cell pattern formation showing that graded cells can be generated by cell behavior involving differences in intercellular repulsion [20]. To discuss such graded cells, the above-mentioned multishell models fail to apply. It is thus necessary to develop a new theory to study the effective properties of graded composite materials under externally applied fields. In a recent work [21], we succeeded in deriving the dipole factor after putting forth a differential effective dipole approximation (DEDA). In this work, we generalize DEDA to nonspherical particles and apply it to investigate the ER spectrum of graded particles in an attempt to investigate their dielectric behavior. Finally, to demonstrate the validity of our model, we fit our theory to experimental data [22] and find good agreement.

II. FORMALISM

We consider an inhomogeneous biological cell or a particle of radius a with complex dielectric constant profile $\widetilde{\epsilon}_1(r)$, embedded in a host fluid of dielectric constant $\widetilde{\epsilon}_2$. Here $\widetilde{\epsilon} = \epsilon + \sigma/(2\pi i f)$, where ϵ denotes real part of the dielectric constant, σ stands for conductivity, f is the frequency of an external field, and $i = \sqrt{-1}$. The dipole factor reflects the polarization of a particle in surrounding medium.

In a recent work [21], we derived the dipole factor for spherical particles by introducing a DEDA. The idea of DEDA can be summarized as follows: Consider a shell model for an inhomogeneous particle. In DEDA one adds new shells of infinitesimal thickness to the particle under consideration. Each of these cells have distance dependent dielectric constant. As the thickness of the layer approaches zero, i.e., $dr \rightarrow 0$, then the correction to the dipole factor due to it is infinitesimal and one can obtain a differential equation for it—hence the name differential effective dipole approximation. Next we extend DEDA to the general case of graded spheroidal particles. Then, we study the effect of different conductivity and dielectric profiles to the electrorotation spectrum, and finally compare the theory to experiments.

We first consider a homogeneous dielectric spheroid in a uniform electric field. The spheroidal inclusion has a dielectric constant $\widetilde{\epsilon}_1$ and it is embedded in a host medium of dielectric constant $\widetilde{\epsilon}_2$. A spheroidal particle can be parametrized by $x^2 + y^2 + (z/h)^2 = r^2$ and the dielectric profile for the graded particle is given by $\widetilde{\epsilon}(r)$, where $0 < r \leq a'$ and h is the aspect ratio and a' is the length of the semiprinciple

axis along $x(y)$ axis. It is worth noting that $h > 1$ denotes a prolate spheroid, whereas $h < 1$ indicates an oblate one. We assume that the longest axis of the spheroid is along the z axis with the depolarization factor L_z, satisfying a sum rule $L_z + 2L_{xy} = 1$ where $L_{x(y)}$ is the depolarization factor along $x(y)$ axis. Regarding the exact relation between L_z and h, we refer the reader to Ref. [23]. For a homogeneous spheroid, the dipole factor along the z axis b_z is given by

$$b_z = \frac{1}{3} \frac{\widetilde{\epsilon}_1 - \widetilde{\epsilon}_2}{\widetilde{\epsilon}_2 + L_z(\widetilde{\epsilon}_1 - \widetilde{\epsilon}_2)}, \tag{1}$$

which measures the degree of polarization for a particle in an external field. Next, we add a confocal spheroidal shell of dielectric constant $\widetilde{\epsilon}$ to the spheroidal particle to make a coated spheroid. Then, the dipole factor of the coated spheroid is [24,25]

$$b_{1z} = \frac{1}{3} \frac{(\widetilde{\epsilon} - \widetilde{\epsilon}_2) + 3x_1\rho[\widetilde{\epsilon} + L_z(\widetilde{\epsilon}_2 - \widetilde{\epsilon})]}{[\widetilde{\epsilon}_2 + L_z(\widetilde{\epsilon} - \widetilde{\epsilon}_2)] + 3x_1\rho L_z(1 - L_z)(\widetilde{\epsilon} - \widetilde{\epsilon}_2)}, \tag{2}$$

where ρ is the volume ratio of the core with respect to the whole spheroid, and

$$x_1 = \frac{1}{3} \frac{\widetilde{\epsilon}_1 - \widetilde{\epsilon}}{\widetilde{\epsilon} + L_z(\widetilde{\epsilon}_1 - \widetilde{\epsilon})}.$$

This approach can be extended to more shells of different dielectric constants, at the expense of obtaining more complicated expressions. It is easy to check that b_{1z} [Eq. (2)] reduces to b_z [Eq. (1)] when $\widetilde{\epsilon} = \widetilde{\epsilon}_1$. Thus, the dipole factor remains unchanged if one adds a spheroidal shell of the same dielectric constant.

Next, we consider an inhomogeneous spheroid with the dielectric profile $\widetilde{\epsilon}(r)$. To establish DEDA, we mimic the graded profile by a multishell construction by building up a dielectric profile by gradually adding shells. We start with an infinitesimal spheroidal core of dielectric constant $\widetilde{\epsilon}(0)$ and continue to add confocal spheroidal shells of dielectric constant $\widetilde{\epsilon}(r)$ until $r = a'$ is reached. At r, we have an inhomogeneous spheroid. To establish a functional form, we replace the inhomogeneous spheroid by a homogeneous spheroid of the same dipole factor, and the graded profile is replaced by an effective dielectric constant $\bar{\epsilon}(r)$. Thus, Eq. (1) becomes

$$b_z(r) = \frac{1}{3} \frac{\bar{\epsilon}(r) - \widetilde{\epsilon}_2}{\widetilde{\epsilon}_2 + L_z(\bar{\epsilon}(r) - \widetilde{\epsilon}_2)}. \tag{3}$$

Next, we add a confocal spheroidal shell of infinitesimal thickness dr, and dielectric constant $\widetilde{\epsilon}(r)$. The dipole factor will change according to Eq. (2). The effective dielectric constant $\bar{\epsilon}(r)$, being related to $b_z(r)$, will also change. To see this, let us write $b_{1z} = b_z + db_z$ and take the limit $dr \rightarrow 0$. We obtain a differential equation:

$$\frac{db_z}{dr} = -\frac{1}{r\widetilde{\epsilon}_2\widetilde{\epsilon}(r)}[\widetilde{\epsilon}_2(1+3b_zL_{1z})-(1-3L_zb_z)\widetilde{\epsilon}(r)]$$

$$\times[\widetilde{\epsilon}_2L_z(1+3b_zL_{1z})+L_{1z}(1-3b_zL_z)\widetilde{\epsilon}(r)], \quad (4)$$

where $L_{1z}=1-L_z$. The dipole factor of a graded spheroidal particle can be calculated by solving the above differential equation with a given gradation profile $\widetilde{\epsilon}(r)$. This nonlinear first-order differential equation can be integrated, at least numerically, if we are given a profile for $\widetilde{\epsilon}(r)$ and an initial condition for $b_z(r=0)$. It is worth noting that the dipole factor is a tensorial quantity and the dipole factor along $x(y)$ axis $b_{x(y)}$ can be obtained by changing L_z to $L_{x(y)}$ in the equation above. It is important to note that substituting $L_z = 1/3$ into this equation yields the DEDA equation for spherical graded particles [21],

$$\frac{db}{dr} = -\frac{1}{3r\widetilde{\epsilon}_2\widetilde{\epsilon}_1(r)}[(1+2b)\widetilde{\epsilon}_2-(1-b)\widetilde{\epsilon}_1(r)]$$

$$\times[(1+2b)\widetilde{\epsilon}_2+2(1-b)\widetilde{\epsilon}_1(r)], \quad (5)$$

where $0<r\leq a$, and a is the radius of the spherical particle. This is the expression we will use in our studies of the effect of conductivity and dielectric profiles on the ER spectrum.

The dipole factor of a graded spherical particle can be calculated by solving the above nonlinear first-order differential equation [Eq. (5)] with a given profile $\widetilde{\epsilon}_1(r)$ and the initial condition

$$b(r=0) = \frac{\widetilde{\epsilon}_1(0)-\widetilde{\epsilon}_2}{\widetilde{\epsilon}_1(0)+2\widetilde{\epsilon}_2}. \quad (6)$$

If we apply a rotating field to the system, a torque between induced dipole moment inside the cell and the electric field vector will set the cell in a rotational motion. It is well known that the frequency-dependent rotation speed $\Omega(f)$ is proportional to the imaginary part of the dipole factor $-\text{Im}[b(r=a)]$. The rotation speed is given by

$$\Omega(f) = -\frac{\epsilon_2 E_0^2}{2\eta}\text{Im}[b(r=a)], \quad (7)$$

where E_0 is the magnitude of the rotating field and η is the viscosity of the host fluid. Hence, when $b(r=a)$ is solved by integrating Eq. (5), we can investigate the electrorotation spectrum.

In order to perform numerical calculations, we take the conductivity and dielectric profiles to be

$$\sigma_1(r) = \sigma_1(0)(r/a)^n, \quad r\leq a,$$

$$\epsilon_1(r) = \epsilon_1(0)+c(r/a), \quad r\leq a,$$

where n and c are profile dependent constants. The profile is quite physical in the sense that the conductivity can change rapidly near the boundary of cell and a power-law profile prevails. The profile constant n can take any positive values and it can be larger than unity. From the above equations it is clear that the conductivity is largest at the boundary. This is the case in real systems as well, since the outermost shell
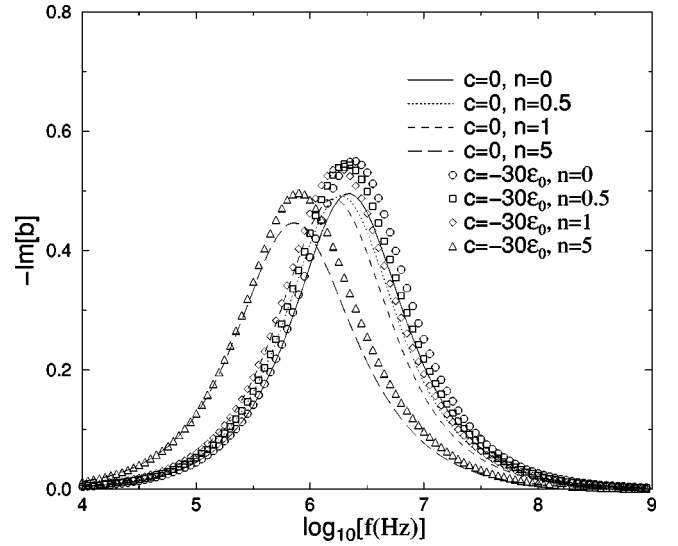

FIG. 1. ER spectrum for profile constants n at $c=0$ and $c=-30\epsilon_0$, respectively. The spectrum is given as the imaginary part of the dipole factor.

(e.g., cell wall) of a cell is always conductive and often has the largest conductivity. On the other hand, the dielectric constant may vary only slightly and thus a linear profile suffices. In particular, the dielectric constant at the center, i.e., $\epsilon_1(0)$, may be larger than that at the boundary. Thus, we will choose $c\leq 0$. By integrating the dielectric profile, we obtain an average dielectric constant ϵ_{av} for different values of c by using a volume average:

$$\epsilon_1^{av} = \frac{\int_0^a \epsilon_1(r)r^2\,dr}{\int_0^a r^2\,dr}. \quad (8)$$

For the present dielectric profile, we obtain $\epsilon_1^{av}=\epsilon_1(0)+3c/4$.

III. NUMERICAL RESULTS

We are now in a position to perform numerical calculations. We set $\sigma_1(0)=2.8\times10^{-2}$ S/m, $\epsilon_1(0)=75\epsilon_0$, $\epsilon_2=80\epsilon_0$, $\sigma_2=2.8\times10^{-4}$ S/m for all of the computations. Parameter ϵ_0 denotes the dielectric constant of vacuum. Here, the numerical results and the comparison to experimental data are limited to spherical cells only, since we were not able to find appropriate experimental data describing nonspherical cells. For the numerical computations, we used the fourth-order Runge-Kutta algorithm with step size 0.01 to solve the above nonlinear first-order differential equation [Eq. (5)]. It was verified that this step size guarantees accurate numerics.

In Fig. 1, the ER spectrum is investigated for various indices n with profile parameters $c=0$ and $c=-30\epsilon_0$. This corresponds to $\epsilon_1^{av}=75\epsilon_0$ and $52.5\epsilon_0$ calculated using Eq. (8), respectively. Figure 1 shows that the rotation peak is always present. It is important to note that the characteristic frequency at which the rotation speed reaches its maximum
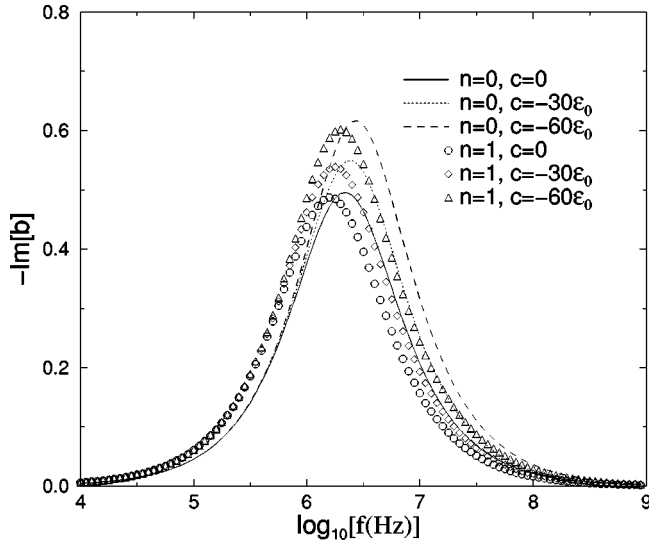
FIG. 2. Same as in Fig. 1, but for various c at $n=0$ and $n=1$, respectively.
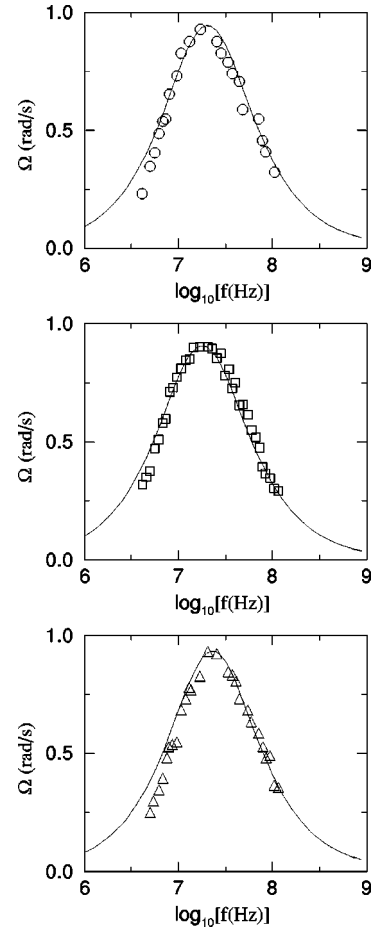

FIG. 3. Fitting of experimental ER spectrum of a yeast cell. The data are extracted from Ref. [22]. The symbols denote experimental data that are measured in water at the beginning, after 20 min, and after 40 min, respectively. The corresponding line denotes the results using the present model.

may be redshifted, i.e., shifted to lower frequencies, especially at large n (e.g., $n=5$) in comparison with small n. Thus, the conclusion is that large fluctuations in conductivity of graded particles may lead to a redshift of the characteristic frequency.

In Fig. 2, the ER spectrum is investigated for $n=0$ and $n=1$, using various slopes c. We use $c=0$, $c=-30\epsilon_0$, and $c=-60\epsilon_0$ corresponding to $\epsilon_1^{av}=75\epsilon_0$, $52.5\epsilon_0$, and $30\epsilon_0$, respectively. From the figure, it is evident that large spatial fluctuations in the dielectric constant may enhance the rotation peak.

From Figs. 1 and 2, we find that spatial conductivity fluctuations are able to make the characteristic frequency redshifted and have a clear effect on the rotation peak. In contrast, spatial dielectric constant fluctuations may enhance the peak value, but their effect on the characteristic frequency is very small. To summarize, we can theoretically obtain a typical ER spectrum with lower characteristic frequency and high rotation speed by adjusting conductivity and dielectric profiles. This corresponds to the physical situation in the case of graded particles.

In Figs. 1 and 2, the particles under consideration are spherical, i.e., $L_z=1/3$. We should remark here that for nonspherical particles, e.g., prolate $0<L_z<1/3$ and oblate spheroids $1/3<L_z<1$, the same conclusions hold (no figures shown here). In addition, it is also found that for prolate (oblate) graded particles, smaller (larger) depolarization factor (L_z) can make the characteristic frequency significantly redshifted.

Finally, to demonstrate our theory, we fit our theory to experimental data in Fig. 3. The data for yeast cells are extracted from the experiments of Reichle *et al.* [22]. In Fig. 3, from upper panel to lower panel, the symbols denote experimental data of the ER spectrum of a yeast cell in water measured at the beginning of the experiment, after 20 min, and after 40 min, respectively. The corresponding continuous lines are the fitted results using the present theory. As discussed earlier, the assumption of homogeneous compart-

ments is not generally justified for biological cells, and the cytoplasm often contains organelles or vacuoles. For this reason, the experimental data are typically fitted using a (two-)shell model. To improve fitting using cell models, one would have to adjust six parameters, i.e., real dielectric constant and conductivity of two shells, as well as cell interior. In contrast, using our theory, only two parameters need to be adjusted, namely, the profile parameters c and n.

For all of the three fittings, we set $\epsilon_2=80\epsilon_0$, $\sigma_2=1.1\times10^{-3}$ S/m (from the experiment), $\epsilon_1(0)=75\epsilon_0$, $\sigma_1(0)=0.28$ S/m, $E_0=10$ kV/m (from experiments), $\eta=2.082\times10^{-2}$ kg/(ms), and $a=5$ μm (given by experiment). For the upper panel, $c=-30\epsilon_0$ (namely, $\epsilon_1^{av}=52.5\epsilon_0$) and $n=0.5$. For the middle panel, $c=-20\epsilon_0$ ($\epsilon_1^{av}=60\epsilon_0$) and $n=0.8$. For the lower panel, $c=-25\epsilon_0$ ($\epsilon_1^{av}=56.25\epsilon_0$) and $n=0.05$.

As seen in Fig. 3, our theory performs very well. Due to the inhomogeneous compartments of a yeast cell, we believe that the graded cell model is a very good choice.

IV. DISCUSSION AND CONCLUSIONS

In this paper, we have generalized the DEDA to nonspherical particles. This allows studies of shape effects, and

indeed colloidal suspensions and many kinds of cells have nonspherical shapes, e.g., red blood cells are oblate spheroids. In particular, for oblate spheroids larger depolarization factor leads to a redshift of the characteristic frequency, for prolate spheroids the systems behave the opposite way [14]. To check the validity of DEDA, it was compared against exact solutions that can be obtained for a power-law profile [26] and a linear profile [27] by solving the Laplace equation for the local electric field. In both cases DEDA produced the same results thus showing that it is essentially exact.

In this paper, we have applied DEDA to discuss the electrorotation spectrum of graded colloidal suspension in an attempt to discuss its dielectric behavior. As a result, we find that changes in the conductivity profile can affect both the characteristic frequency (redshift) and rotation peak, whereas changes in the dielectric profile may enhance the rotation peak only. Consequently, we may conclude that the graded behavior does play an important role in the dielectric properties of graded suspensions. We used our theory (for spherical cells) to fit results obtained by Reichle *et al.* [22] for yeast cells and obtained excellent agreement. It would be interesting to compare this theory to experimental results for nonspherical cells as well, and hopefully new experiments will be performed in that direction.

The inhomogeneous structure will give rise to a whole wealth of dispersions inside the cells. The additional dispersions due to a graded profile will not only affect the dielectric dispersion of cells, but it also changes the behavior of electro-orientation. A detailed analysis of the behavior is not possible without a model that enables us to reveal the complete information of the dispersions arising from the inhomogeneous structure. Foster *et al.* discussed the case in which particles with an intrinsic dispersion were embedded in a nondispersive medium [28]. These authors analyzed a model in which one single dispersion is associated with the suspended particles, however, neither mentioning the origin of the dispersion nor the detailed information on the possible inhomogeneous cell structure.

Our work may be extended to discuss the ER spectrum of a pair of particles by taking into account the multiple image effect [29,30] and to investigate high concentration suspensions by discussing the local-field effects [31,32]. A generalization which includes both of these effects is of particular interest. In addition to the ER spectrum, our theory may be used to discuss other electrokinetic effects, e.g., dielectrophoresis [33,30] and electro-orientation [34].

[1] C. Dalton, A.D. Goater, J. Drysdale, and R. Pethig, Colloids Surf., A **195**, 263 (2001).

[2] Y.H. Jun Yang, X.-B. Wang, F.F. Becker, and P.R.C. Gascoyne, Biophys. J. **78**, 2680 (2000).

[3] M.P. Hughes, Nanotechnology **11**, 124 (2000).

[4] M.P. Hughes, Nanotechnology **13**, 157 (2002).

[5] K.L. Chan, P.R.C. Gascoyne, F.F. Becker, and R. Pethig, Biochim. Biophys. Acta **1349**, 182 (1997).

[6] W.M. Arnold and U. Zimmermann, Z. Naturforsch. C **37**, 908 (1982).

[7] V.P. Pastushenko, P.I. Kuzmin, and A.Y. Chizmadshev, Stud. Biophys. **110**, 51 (1985).

[8] J. Gimsa, T. Muller, T. Schnellea, and G. Fuhr, Biophys. J. **71**, 495 (1996).

[9] A.A. Teixera-Pinto, L.L. Nejelski, J.L. Cutler, and J.H. Heller, Exp. Cell Res. **20**, 548 (1960).

[10] G. Fuhr, U. Zimmermann, and S. Shirley, *Electromanipulation of Cells* (CRC Press, Boca Raton, FL, 1996), pp. 259–328.

[11] J. Yang, Y. Huang, X. Wang, X.B. Wang, F. Becker, and P.R.C. Gascoyne, Biophys. J. **76**, 3307 (1999).

[12] F.F. Becker, X.B. Wang, Y. Huang, R. Pethig, J. Vykoukal, and P.R.C. Gascoyne, Proc. Natl. Acad. Sci. U.S.A. **92**, 860 (1995).

[13] K.L. Chan, H. Morgan, E. Morgan, I.T. Cameron, and M.R. Thomas, Biochim. Biophys. Acta **1500**, 313 (2000).

[14] J.P. Huang and K.W. Yu, J. Phys.: Condens. Matter **14**, 1213 (2002).

[15] J. Gimsa, Bioelectrochemistry **54**, 23 (2001).

[16] H. Fricke, Phys. Rev. **26**, 682 (1925).

[17] G. Fuhr and P.I. Kuzmin, Biophys. J. **50**, 789 (1986).

[18] S. Suresh, Science (Washington, DC, U.S.) **292**, 2447 (2001).

[19] A.M. Freyria, E. Chignier, J. Guidollet, and P. Louisot, Biomaterials **12**, 111 (1991).

[20] H. Honda and A. Mochizuki, Dev. Dyn. **223**, 180 (2002).

[21] K.W. Yu, G.Q. Gu, and J.P. Huang, e-print cond-mat/0211532.

[22] C. Reichle, T. Schnelle, T. Muller, T. Leya, and G. Fuhr, Biochim. Biophys. Acta **1459**, 281 (2000).

[23] W.T. Doyle and I.S. Jacobs, J. Appl. Phys. **71**, 3926 (1992).

[24] L. Gao, J.T.K. Wan, K.W. Yu, and Z.Y. Li, J. Phys.: Condens. Matter **12**, 6825 (2000).

[25] P. Sheng, Phys. Rev. Lett. **45**, 60 (1980).

[26] G.Q. Gu and K.W. Yu (unpublished).

[27] L. Dong and K.W. Yu (unpublished).

[28] K.R. Foster, F.A. Sauer, and H.P. Schwan, Biophys. J. **63**, 180 (1992).

[29] J.P. Huang, K.W. Yu, and G.Q. Gu, Phys. Rev. E **65**, 021401 (2002).

[30] J.P. Huang, M. Karttunen, K.W. Yu, and L. Dong, Phys. Rev. E **67**, 021403 (2003).

[31] J.P. Huang, K.W. Yu, and G.Q. Gu, Phys. Lett. A **300**, 385 (2002).

[32] L. Gao, J.P. Huang, and K.W. Yu, Phys. Rev. E **67**, 021910 (2003).

[33] H.A. Pohl, *Dielectrophoresis* (Cambridge University Press, Cambridge, 1978).

[34] M. Saito, H.P Schwan, and G. Schwarz, Biophys. J. **6**, 313 (1966).